

Galerkin approximations for dissipative magnetohydrodynamics

Hudong Chen, Xiaowen Shan, and David Montgomery

Department of Physics and Astronomy, Dartmouth College, Hanover, New Hampshire 03755

(Received 15 May 1990)

A Galerkin approximation scheme is proposed for voltage-driven, dissipative magnetohydrodynamics. The trial functions are exact eigenfunctions of the linearized continuum equations and represent helical deformations of the axisymmetric, zero-flow, driven steady state. In this paper, the lowest nontrivial truncation is explored: one axisymmetric trial function and one helical trial function each for the magnetic and velocity fields. The system resembles the Lorenz approximation to Bénard convection, but in the region of believed applicability its dynamical behavior is rather different, including relaxation to a helically deformed state similar to those that have emerged in the much higher resolution computations of Dahlburg *et al.* [Phys. Rev. Lett. **57**, 428 (1986); J. Plasma Phys. **37**, 299 (1987); **40**, 39 (1988)]. In the region of applicability, the dynamical behavior is to seek out the steady state of lowest energy dissipation rate.

I. INTRODUCTION

Only a limited amount of information about driven, dissipative continuum systems is available from low-order Galerkin approximations. Consider, for example, the three-mode approximation of Lorenz for the Bénard convection problem.¹ It can be said without too much exaggeration to have spawned an entirely new branch of dynamical systems theory, yet its predictions have to be drastically revised as the number of modes increases toward a well-resolved solution (see, e.g., Curry² and Curry *et al.*³). Clarifying the relation between low-order Galerkin approximations⁴ and true continuum behavior is one of the more urgent problems in nonlinear mechanics, if we hope to learn much about the latter from the former.

One purpose here is to present an alternative Galerkin approximation scheme for a plasma-magnetohydrodynamic system of some recent interest in connection with plasma confinement.⁵⁻⁹ We then explore the consequences of the scheme for the lowest-order nontrivial truncation. The system bears some strong formal resemblance to the Bénard problem, though the underlying physics is different. We consider a resistive, viscous magnetofluid contained in a rigid cylinder with periodically identified ends (to simulate a toroidal confinement device). An externally imposed dc magnetic field points in the axial (z) direction, and an electric current is driven along it by an applied axial voltage (in the laboratory setting, this is often an inductively driven toroidal electric field). There is an analogy between the applied axial voltage drop and the applied temperature drop in the Bénard problem; the electric current is an analogue of the Bénard heat current. In both cases, when the enforced gradients reach critical values, expressible in terms of characteristic dimensionless ratios of the problem, the quiescent state that had prevailed up to the threshold becomes linearly unstable and gives way to one involving fluid motion.

The magnetohydrodynamic (hereafter, MHD) problem has the pleasant feature that the linear eigenfunctions of the quiescent state which become unstable are explicitly

calculable⁷ and can be used as an orthonormal basis of "trial functions" for the Galerkin approximation.⁴ This must be viewed as a lucky accident that is not shared by many of the threshold-unstable continuum problems to which one might think of applying Galerkin techniques, though the expansion functions of the Lorenz problem with free-slip boundary conditions are exact eigenfunctions.

It will be seen how similar in structure a three-mode truncation of the above MHD problem is to the Lorenz model. Indeed, for a particular choice of parameters, the three-mode MHD problem reduces to the Lorenz model and in a surrounding range, exhibits strange attractors and other "chaotic" phenomena. However, away from this special set of parameters and in what is very probably a more physically relevant regime, there is a qualitative change in the dynamical behavior of the three-mode truncation and no Lorenzian behavior is exhibited. The strange attractors and "chaos" are only attainable by pushing the model beyond its likely realm of physical applicability.

Another purpose of this article is to propose a framework for a future intended attack on the MHD problem using Galerkin approximations of much higher order. A truism of much of computational fluid mechanics is that spectral or pseudospectral codes are more efficient for large computations than pure, transform-space, Galerkin methods because of the need to evaluate many lengthy convolution sums in the latter.⁴ The disparity becomes greater the higher the Reynolds-like numbers. However, certain features of the MHD problem arise that make the arguments less conclusive there, and we wish now to review these.

First, the fluid problems solved, such as plane Poiseuille flow, plane Couette flow, Bénard convection, etc., have been such as to lend themselves to treatment with rectangular boundary conditions defined by channels, slabs, and spatially periodic directions. All are problems in which little of importance gets lost by the restriction to rectangular symmetries. However, the prob-

lem of pipe flow has apparently proved less tractable, at least in part because of complications from the on-axis singularities ($r=0$ in cylindrical polar coordinates). For the cylinder of voltage-driven magnetofluid, with its helical magnetic field lines and normal modes, the cylindrical character of the problem is of the essence. The problem can be in danger of being reduced to a caricature of itself by rectangular simplifications. Other magnetofluid codes have implicitly conceded this point by a somewhat artificial avoidance of situations in which much of anything is allowed to happen at $r=0$.

Finally, even if laboratory values of Lundquist and Reynolds numbers may not be approachable in pure Galerkin-approximation computations, there is so little accurate information (experimental or computational) about driven, dissipative MHD systems that there still seems to be something to be learned about threshold behavior at even modest values of the Reynoldslike numbers. In summary, the advantages of a Galerkin computation might be as follow: (1) no problems associated with singularities arise at or near $r=0$, however violent the behavior, (2) the expansion functions will all automatically obey the boundary conditions and maintain the solenoidal property of the fields; and (3) even at relatively low Reynolds-like numbers, a great many only recently opened issues of transition behavior in driven, dissipative (as contrasted with ideal) MHD remain to be resolved. Unlike fluid mechanics, whose laminar flows, thresholds for instability, and transition behaviors may be considered rather well understood, the preturbulent states of MHD and their transition behavior are far from a settled matter. Nor is it clear how much of a role fully developed MHD turbulence actually plays in the magnetically supported driven steady state after the formation phase.⁵

An outline of the paper follows. Section II sets out the MHD equations and the expansion basis in which they are to be solved: the Chandrasekhar-Kendall orthonormal eigenfunctions of the curl.¹⁰ Both the magnetohydrodynamics (scalar, one-fluid, incompressible, with scalar transport coefficients) and the boundary conditions are admittedly oversimplified, on the assumption that, even with the oversimplifications, the system is complicated enough. The boundary conditions at the confining cylinder wall are $\mathbf{B} \cdot \hat{\mathbf{n}}=0$, $\mathbf{j} \cdot \hat{\mathbf{n}}=0$, $\mathbf{v} \cdot \hat{\mathbf{n}}=0$, $\boldsymbol{\omega} \cdot \hat{\mathbf{n}}=0$, where $\hat{\mathbf{n}}=\hat{\mathbf{e}}_r$ is the unit normal at the wall $r=a$. \mathbf{B} is the magnetic field, \mathbf{j} is the electric current density, \mathbf{v} is the velocity field, and $\boldsymbol{\omega}=\nabla \times \mathbf{v}$ is the vorticity. The boundary conditions on \mathbf{B} , \mathbf{j} , and \mathbf{v} are those appropriate to a rigid, impenetrable, perfectly conducting wall coated with a thin layer of insulating dielectric. The fourth boundary condition, $\boldsymbol{\omega} \cdot \hat{\mathbf{n}}=0$, is less than wholly satisfactory, but replacing it with either "no-slip" or "stress-free" mechanical boundary conditions from fluid mechanics has seemed, so far, to move the problem out of reach.⁷ The observation that in the MHD computations, most of the mechanical activity seems to occur away from the wall⁵ allows us to hope that the approximation is not disastrous.

Section III sets out the analytical machinery for the three-mode Galerkin approximation and describes some numerical solutions of it. Its similarity to the Lorenz

problem is remarked upon, as is the matter of a lowered dissipation rate⁷ in establishing the steady helical state above the instability threshold. Section IV is a summary and suggests possible future computations involving many-mode Galerkin approximations.

II. EXPANSION IN CHANDRASEKHAR-KENDALL FUNCTIONS

The equations of incompressible MHD are, in a familiar set of dimensionless variables ("Alfvénic" units):

$$\frac{\partial \mathbf{v}}{\partial t} = \mathbf{v} \times \boldsymbol{\omega} + \mathbf{j} \times \mathbf{B} - \nabla p^* - \nu \nabla^2 \mathbf{v}, \quad (1)$$

$$\frac{\partial \mathbf{B}}{\partial t} = \nabla \times (\mathbf{v} \times \mathbf{B}) - \eta \nabla^2 \mathbf{j}, \quad (2)$$

$$\nabla \cdot \mathbf{v} = 0, \quad (3)$$

$$\nabla \cdot \mathbf{B} = 0. \quad (4)$$

In Eqs. (1)–(4), \mathbf{v} and \mathbf{B} are the velocity field and magnetic field, respectively, while the electric current density is $\mathbf{j}=\nabla \times \mathbf{B}$ and the vorticity is $\boldsymbol{\omega}=\nabla \times \mathbf{v}$. The mechanical pressure is p , and $p^*=p+\mathbf{v}^2/2$. p^* is obtained by taking the divergence of Eq. (1) and solving the Poisson equation which results when we note $\nabla \cdot (\partial \mathbf{v} / \partial t) = 0$, by Eq. (3). The dimensionless viscosity ν and dimensionless magnetic diffusivity η are taken to be uniform constants and may be thought of as the reciprocals of Reynolds-like numbers. Equations (1)–(4) are written without reference to the applied electric field; inclusion of the applied electric field or voltage will be discussed later.

The expansion functions to be used in expressing the solenoidal fields \mathbf{v} and \mathbf{B} are the normalized Chandrasekhar-Kendall eigenfunctions¹⁰ of the curl

$$\nabla \times \mathbf{A}_{nmq} = \lambda_{nmq} \mathbf{A}_{nmq}. \quad (5)$$

\mathbf{A}_{nmq} may be taken to be

$$\mathbf{A}_{nmq} = I_{nmq}^{-1/2} \mathbf{J}_{nmq}, \quad (6)$$

where

$$\mathbf{J}_{nmq} = \lambda_{nmq} \nabla \psi_{nmq} \times \hat{\mathbf{e}}_z + \nabla \times (\nabla \psi_{nmq} \times \hat{\mathbf{e}}_z), \quad (7)$$

with

$$\psi_{nmq} = J_m(\gamma_{nmq} r) \exp(im\phi - ik_n z) \quad (8)$$

in cylindrical coordinates (r, ϕ, z) . Here, J_m is the Bessel function of the first kind of integer order m . The indices are integers, with $n=0, \pm 1, \pm 2, \dots$, $m=0, \pm 1, \pm 2, \dots$, and $q=1, 2, 3, \dots$. The wave number $k_n=2\pi n/L_z$, where L_z is the periodicity length in the axial (z) direction; this is the only concession to the toroidal nature of the problem. λ_{nmq} is $\pm(\gamma_{nmq}^2 + k_n^2)^{1/2}$, with both signs allowed. I_{nmq} is a normalization integral chosen so that

$$\int \mathbf{A}_{nmq}^* \cdot \mathbf{A}_{nmq} d^3x = 1, \quad (9)$$

where the region of volume integration is the interior of the right circular cylinder $0 \leq r \leq a$, $0 \leq z \leq L_z$.

All quantities have now been specified except the γ_{nmq} .

The γ_{nmq} are always greater than or equal to zero and are defined differently from the axisymmetric eigenfunctions \mathbf{A}_{00q} than for the ‘‘helical’’ ones (the \mathbf{A}_{nmq} with $m^2 + n^2 > 0$). For the nonaxisymmetric ones, the boundary condition $\hat{\mathbf{e}}_r \cdot \mathbf{A}_{nmq}(r=a) = 0$ gives

$$\lambda_{nmq} \frac{m}{a} J_m(\gamma_{nmq} a) = k_n \frac{dJ_m(\gamma_{nmq} a)}{da}, \quad (10)$$

which determines an infinite sequence of positive γ_{nmq} for each m and n , $m^2 + n^2 > 0$, and the associated λ_{nmq} of both signs.

For the \mathbf{A}_{00q} , there is no radial component, and some decisions are necessary. One convenient choice is to fix $\gamma_{001} > 0$, and then determine all higher γ_{00q} from the requirement that all the \mathbf{A}_{00q} be orthogonal to \mathbf{A}_{001} and to each other. A second possibility is to demand that the \mathbf{A}_{00q} be ‘‘fluxless,’’ which is achieved by requiring that $\hat{\mathbf{e}}_\phi \cdot \mathbf{A}_{00q}(r=a) = 0$ be used to determine the γ_{00q} and λ_{00q} . This second choice leads to some subtleties in that it requires the introduction of an axisymmetric function orthogonal to all the \mathbf{A}_{00q} to carry the net axial current. Discussion of how to construct this function in detail for arbitrary numbers of retained \mathbf{A}_{00q} will be deferred to a later publication, since it is rather involved and is not needed for the simple three-mode truncation investigated here. Thus the analog of Eq. (9) for $m=0=n$ is just $J'_0(\gamma_{00q} a) = 0$. The normalization integral I_{nmq} is

$$I_{nmq} = 2\pi L_z J_m^2(\gamma_{nmq} a) \times \left[\frac{m \lambda_{nmq} \gamma_{nmq}^2}{k_n} + \lambda_{nmq}^2 (\gamma_{nmq} a)^2 \left(1 + \frac{m^2}{k_n^2 a^2} \right) \right]. \quad (11)$$

With these choices, it may be readily shown that

$$\int \mathbf{A}_{nmq}^* \cdot \mathbf{A}_{n'm'q} d^3x = \delta_{nn'} \delta_{mm'} \delta_{qq'}. \quad (12)$$

The \mathbf{A}_{nmq} constitute a triply infinite orthonormal set for expanding solenoidal fields, analogous to the Fourier series used in discussing homogeneous Navier-Stokes turbulence with periodic boundary conditions. Supplemented by an orthogonal axisymmetric function to carry the net axial current, they may be supposed to be a complete set for expanding solenoidal fields obeying the boundary conditions we are assuming, though it appears that no completeness theorems have been proved. They will be computationally useful only in problems in which the convergence can be assumed to be rather rapid. It will not be true, of course, that superpositions of them are also eigenfunctions of the curl.

We seek a representation of the \mathbf{v} and \mathbf{B} fields of the following form:

$$\mathbf{v} = \sum_{n,m,q} \xi_{nmq}^v \mathbf{A}_{nmq} \quad (13)$$

and

$$\mathbf{B} = B_0 \hat{\mathbf{e}}_z + j_0 \mathbf{A}_0 + \sum_{n,m,q} \xi_{nmq}^B \mathbf{A}_{nmq}. \quad (14)$$

The sums are over all n, m, q , including both signs of

λ_{nmq} . Here, ξ_{nmq}^v and ξ_{nmq}^B are scalar amplitudes and contain the time dependences. The amplitude j_0 is also a function of time, but $B_0 = \text{const}$ is not. The function $\mathbf{A}_0(\mathbf{r})$ is axisymmetric and orthogonal to all the other \mathbf{A}_{nmq} ; for purposes of the three-mode truncation to be considered here, it is simply $\frac{1}{2} r \hat{\mathbf{e}}_\phi$; if the \mathbf{A}_{00q} 's were going to be retained, $\mathbf{A}_0(\mathbf{r})$ would have additional terms. The sums over nmq , in general, run over all allowed values, but here these sums will be drastically truncated.

Upon substitution of Eqs. (13) and (14) into Eq. (2) and the curl of Eq. (1), we take inner products with individual $\mathbf{A}_{nmq}(\mathbf{r})$ and with $\mathbf{A}_0(\mathbf{r})$. The results are of the general form

$$\frac{d\xi_{nmq}^v}{dt} = f_v(\xi^v, \xi^B, j_0), \quad (15)$$

$$\frac{d\xi_{nmq}^B}{dt} = f_B(\xi^v, \xi^B, j_0), \quad (16)$$

$$\frac{dj_0}{dt} = f_j(\xi^v, \xi^B, j_0), \quad (17)$$

where the right-hand sides become known, if complicated, functions of the various amplitudes. By a Galerkin approximation, we shall mean the results of discarding all but N of Eqs. (15)–(17), and all but N of the corresponding amplitudes. These ordinary differential equations govern then the approximation to the dynamics.

To discuss the effect of applying an axial electric field at the wall, we must pull a curl off Eq. (2) and discuss the evolution of the vector potential \mathbf{A} , for which $\mathbf{B} = \nabla \times \mathbf{A}$. We get

$$\frac{\partial \mathbf{A}}{\partial t} = \mathbf{v} \times \mathbf{B} - \eta \mathbf{j} + \mathbf{E}_0 + \nabla \Phi, \quad (18)$$

where Φ is a periodic scalar potential for which (using the Coulomb gauge)

$$\nabla^2 \Phi = -\nabla \cdot (\mathbf{v} \times \mathbf{B}). \quad (19)$$

Φ obeys the boundary condition $\Phi = 0$ at $r = a$. \mathbf{E}_0 is the electric field applied at the wall: $\mathbf{E}_0 = E_0(t) \hat{\mathbf{e}}_z$, where $E_0(t)$ is given. Substituting the expansions into Eq. (18) and spatial averaging then leads to the detailed form of the right-hand side of Eq. (17).

We now truncate Eqs. (15)–(17) drastically. Namely, we keep only one ξ_{nmq}^v , one ξ_{nmq}^B and j_0 . Hereafter, this nmq will be regarded as fixed and known. The result is, after some algebra,

$$\frac{d\xi_{nmq}^v}{dt} = -i \left[k_n B_0 - \frac{mj_0}{2} - \frac{k_n j_0}{\lambda_{nmq}} \right] \xi_{nmq}^B - \nu \lambda_{nmq}^2 \xi_{nmq}^v, \quad (20)$$

$$\frac{d\xi_{nmq}^B}{dt} = -i \left[k_n B_0 - \frac{mj_0}{2} \right] \xi_{nmq}^v - \eta \lambda_{nmq}^2 \xi_{nmq}^B, \quad (21)$$

and

$$\frac{a^2}{8} \frac{dj_0}{dt} = E_0 - \eta j_0 + 2 \text{Re} \left[\frac{ik_n}{\lambda_{nmq}} \frac{\xi_{nmq}^B \xi_{nmq}^{v*}}{\pi a^2 L_z} \right]. \quad (22)$$

The three complex-conjugate relations, involving $\xi_{-n-m,q}^v$ and $\xi_{-n,-m,q}^B$, are also implied but are not independent, since $\xi_{nmq}^{v,B} = \xi_{-n,-m,q}^{v,B*}$, for reality of \mathbf{v} and \mathbf{B} . As previously remarked, Eqs. (20)–(22) involve exactly the dynamics of one linear eigenmode of the uniform-current-density problem, plus its interaction with the spatially-averaged current density j_0 . It is natural to select the n , m , and q as the indices of the first linear normal mode to go unstable as E_0 is raised, at fixed η , ν , L_z , B_0 , and a . This is in fact the physically motivated choice, to allow the first mode that wants to participate in the dynamics the opportunity to do so. However, mathematically there is no necessity for this choice and n, m, q can be the indices of any mode.

A further simplification, that can be achieved without further loss of generality, is to phase the participating helical modes so that

$$\begin{aligned} \frac{1}{2} \xi_{nmq}^B \exp(im\phi - ik_n z) + \text{c. c.} \\ = \left[\frac{\pi a^2 L_z}{2} \right]^{1/2} [X_\alpha \cos(m\phi - k_n z)] \end{aligned}$$

and

$$\begin{aligned} \frac{1}{2} \xi_{nmq}^v \exp(im\phi - ik_n z) + \text{c. c.} \\ = - \left[\frac{\pi a^2 L_z}{2} \right]^{1/2} [Y_\alpha \sin(m\phi - k_n z)] \end{aligned}$$

(where c.c. stands for the complex conjugate), in terms of real amplitudes X_α, Y_α . (The subscript α stands symbolically for the nmq of the retained mode.) Equations (20)–(22) now reduce to the purely real system

$$\frac{dX_\alpha}{dt} = \left[\frac{m_\alpha j_0}{2} - k_\alpha B_0 \right] Y_\alpha - \eta \lambda_\alpha^2 X_\alpha, \quad (23)$$

$$\frac{dY_\alpha}{dt} = - \left[\frac{m_\alpha j_0}{2} - k_\alpha B_0 + \frac{k_\alpha j_0}{\lambda_\alpha} \right] X_\alpha - \nu \lambda_\alpha^2 Y_\alpha, \quad (24)$$

$$\frac{a^2}{8} \frac{dj_0}{dt} = E_0 - \eta j_0 + \frac{k_\alpha}{\lambda_\alpha} X_\alpha Y_\alpha. \quad (25)$$

A cleaner-looking version of Eqs. (23)–(25) results from an additional rescaling of the variables: $\tau \equiv (\sqrt{2}m/a)t$, $\beta_0 \equiv k_n B_0 a / \sqrt{2}m$, $\gamma_0 \equiv 2k_n / m \lambda_{nmq}$, $\nu_0 \equiv \nu \lambda_{nmq}^2 a / \sqrt{2}m$, $\eta_0 \equiv \eta \lambda_{nmq}^2 a / \sqrt{2}m$, $\zeta_0 \equiv 8\eta / \sqrt{2}am$, $Z \equiv a j_0 / 2\sqrt{2}$, and $Z_0 \equiv a E_0 / 2\sqrt{2}\eta$. Dropping the α subscript, we have simply

$$\frac{dX}{d\tau} = (Z - \beta_0)Y - \eta_0 X, \quad (26)$$

$$\frac{dY}{d\tau} = [\beta_0 - (1 + \gamma_0)Z]X - \nu_0 Y, \quad (27)$$

$$\frac{dZ}{d\tau} = \gamma_0 XY - \zeta_0 (Z - Z_0). \quad (28)$$

The quantities with zero subscripts are constants, determined by the physical constants of the problem. For the particular set of parameters that makes $1 + \gamma_0 = 0$, Eqs. (26)–(28) can be reduced to the Lorenz model, but for

any other set of parameters there is an extra nonlinear term in Eq. (27) that breaks the correspondence.

It should be remarked that linearizing Eqs. (20)–(22), (23)–(25), or (26)–(28) about the uniform axisymmetric state $j_0 = E_0 / \eta$, $X = Y = 0$ leads to exactly the same eigenfunctions and dispersion relation as one gets from the full MHD problem.⁷

III. DYNAMICS OF THE THREE-MODE TRUNCATION

Equations (26)–(28), though grossly oversimplifying the full MHD dynamics represented by Eqs. (1)–(4) are still an interesting dynamical system. They have the somewhat unusual feature of having resulted from a Galerkin approximation based on trial functions that are themselves exact eigenfunctions for the axisymmetric equilibrium profile, not just approximations thereto. Perhaps for that reason, numerical integration of Eqs. (26)–(28) reveals that they share some properties of the full MHD equations in some circumstances. In particular, this is the case when parameter regimes are confined to those immediately above (or below) the critical value of j_0 at which the axisymmetric, zero-flow steady state of the full MHD equations first becomes linearly unstable, and when the X and Y amplitudes are taken to correspond to the first n , m , and q that goes linearly unstable.

For the special case $1 + \gamma_0 = 0$, the Z -proportional term drops out of the right-hand side of Eq. (27). Further rescaling will then convert Eqs. (26)–(28) into the exact Lorenz system. For $1 + \gamma_0 \neq 0$, the system's behavior is different from that of the Lorenz model, and for physically motivated parameter choices, exhibits less chaotic behavior.

The externally-fixed driving term in Eqs. (26)–(28) is Z_0 , directly proportional to the applied electric field E_0 . In a region immediately above $Z_0 = 0$, the only steady-state solution is $X = Y = 0$ and $Z = Z_0$. This corresponds to the exact, axisymmetric, uniform-current-density, steady-state solution of Eqs. (1)–(4). In this range of Z_0 , the dynamical behavior of Eqs. (26)–(28), as revealed by numerical solution, is a straightforward relaxation to this “fixed point” (steady state).

At a first critical value of Z_0 (or critical current $j_0 = E_0 / \eta$), the axisymmetric, uniform-current-density state becomes linearly unstable. This critical current corresponds exactly to the value of j_0 obtained as the linear stability threshold from the full set of MHD equations (1)–(4). It is the lesser root in the solution for j_0 in

$$\left[\frac{mj_0}{2} - k_n B_0 \right] \left[\frac{mj_0}{2} - k_n B_0 + \frac{k_n j_0}{\lambda_{nmq}} \right] + \eta \nu \lambda_{nmq}^4 = 0, \quad (29)$$

for any n , m , and q . Equation (29) is the zero-frequency dispersion relation obtained by linearizing about the axisymmetric state. Its stability boundary has been tabulated elsewhere.⁹ The critical current depends only upon the Hartmann number.

A second, stable, fixed point appears at the value of Z_0

at which the axisymmetric solution becomes unstable. This stable fixed point is characterized by a helical contribution which increases as Z_0 increases above its critical value. For this solution, j_0 remains locked at the value given by Eq. (29), and the helical components act as an “anomalous resistance,” or back emf, which opposes E_0 . From Eq. (25), j_0 stays at a constant value

$$\eta j_0 = E_0 + \frac{k_\alpha}{\lambda_\alpha} X_\alpha Y_\alpha, \tag{30}$$

while E_0 and the (negative) second term on the right-

hand side grow in absolute value together. In this state, increasing E_0 increases the helical distortion but does not increase the net plasma current.

If the first linearly unstable eigenmode is used to determine the n, m, q that identify X and Y , the helical state is a stable attractor in a finite range of Z_0 above its appearance, while the axisymmetric state becomes unstable and ceases to function as an attractor. The helical state is degenerate under $X \rightarrow -X, Y \rightarrow -Y$, and its stability in a finite range above the critical E_0 can be proved algebraically.

Behavior of the kind just described is illustrated by

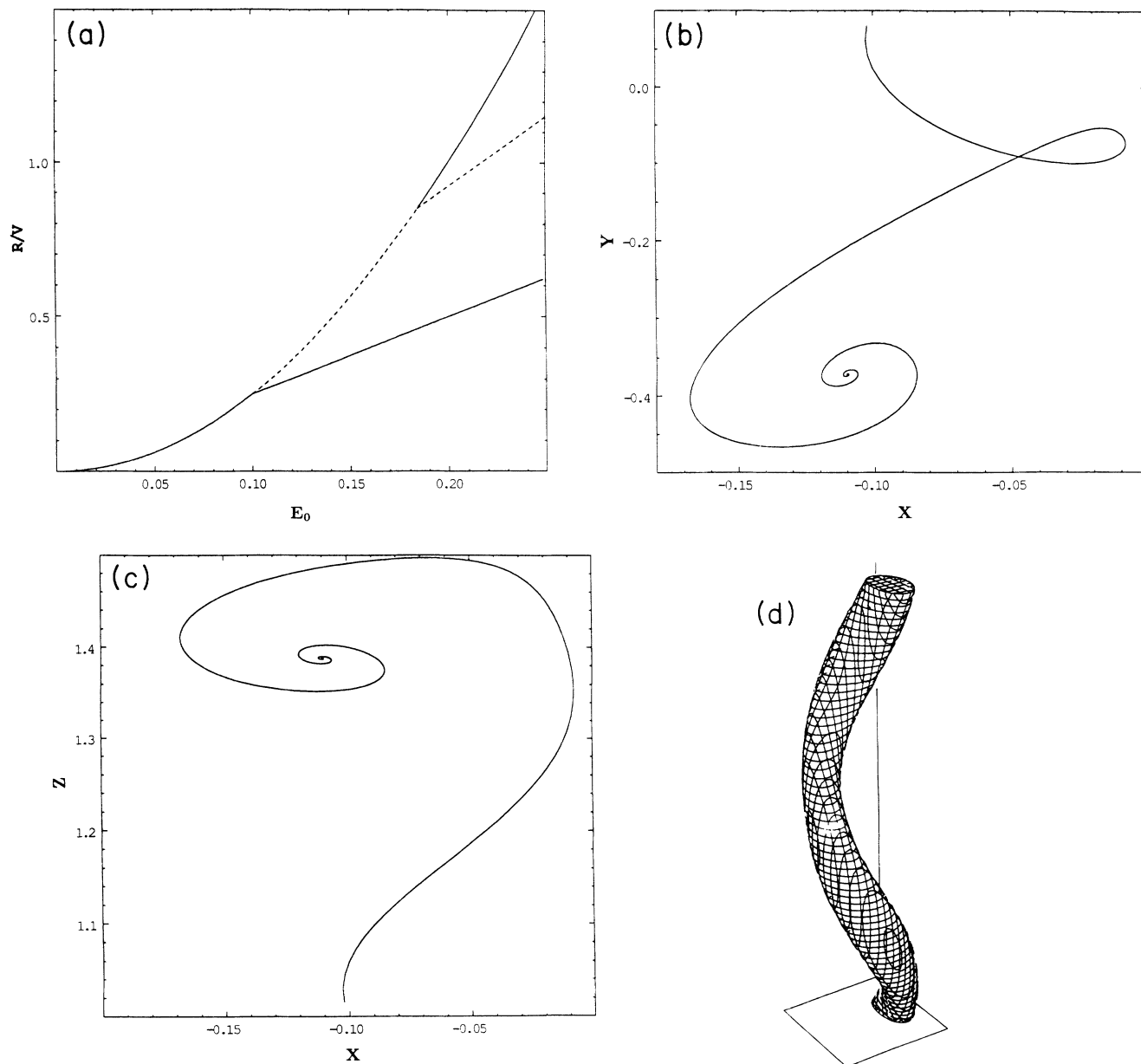


FIG. 1. (a) Total-energy dissipation rate per unit volume vs applied electric field for the steady states of Eqs. (26)–(28). Solid curves correspond to stable fixed points and dashed curves to unstable ones. (b) Relaxation to a helical fixed point for the situation in (a), for an E_0 10% greater than its critical value, in the XY plane. (c) Relaxation to a helical fixed point in the XZ plane for the same case as (b). (d) Computer-drawn surface of constant $j_z(x,y,z) = 2.7$ for the helical state to which the relaxation in (b) and (c) occurs.

Fig. 1. The parameters relevant to Fig. 1 are $L_z = 4\pi$, $a = \pi/2$, $B_0 = 2.4$, $\eta = \nu = 0.04$. The first linearly unstable mode is $m = 1$, $n = 1$, $q = 1$, $\lambda a = -3.2069$. The critical E_0 is 0.1, while the threshold j_0 is 2.5. Figure 1(a) is a plot of total dissipation per unit volume versus E_0 in the original, Alfvénic, units. The parabola is E_0^2/η , the Ohmic dissipation associated with the axisymmetric state. At $E_0 = 0.1$, the first helical fixed point appears and the dissipation of this state depends linearly upon E_0 , rather than quadratically. Solid lines indicate stable steady states, while dashed lines indicate unstable ones. The attracting, stable, helical solution is characterized by

a lower total dissipation (for the same E_0) than the unstable axisymmetric state in a range above the critical E_0 . At a second critical E_0 , given by solving Eq. (29) for j_0 and replacing j_0 by E_0/η in the larger root, a second helical fixed point appears and, as may also be demonstrated by explicit algebra, is always unstable; it is indicated by the (dashed) upper straight line in Fig. 1(a). After its appearance, both the axisymmetric state and the first helical state are stable and attracting, with an apparently rather complicated boundary between their basins of attraction. By the time this value of E_0 is reached, there is probably no reason to expect Eqs. (26)–(28) to represent Eqs.

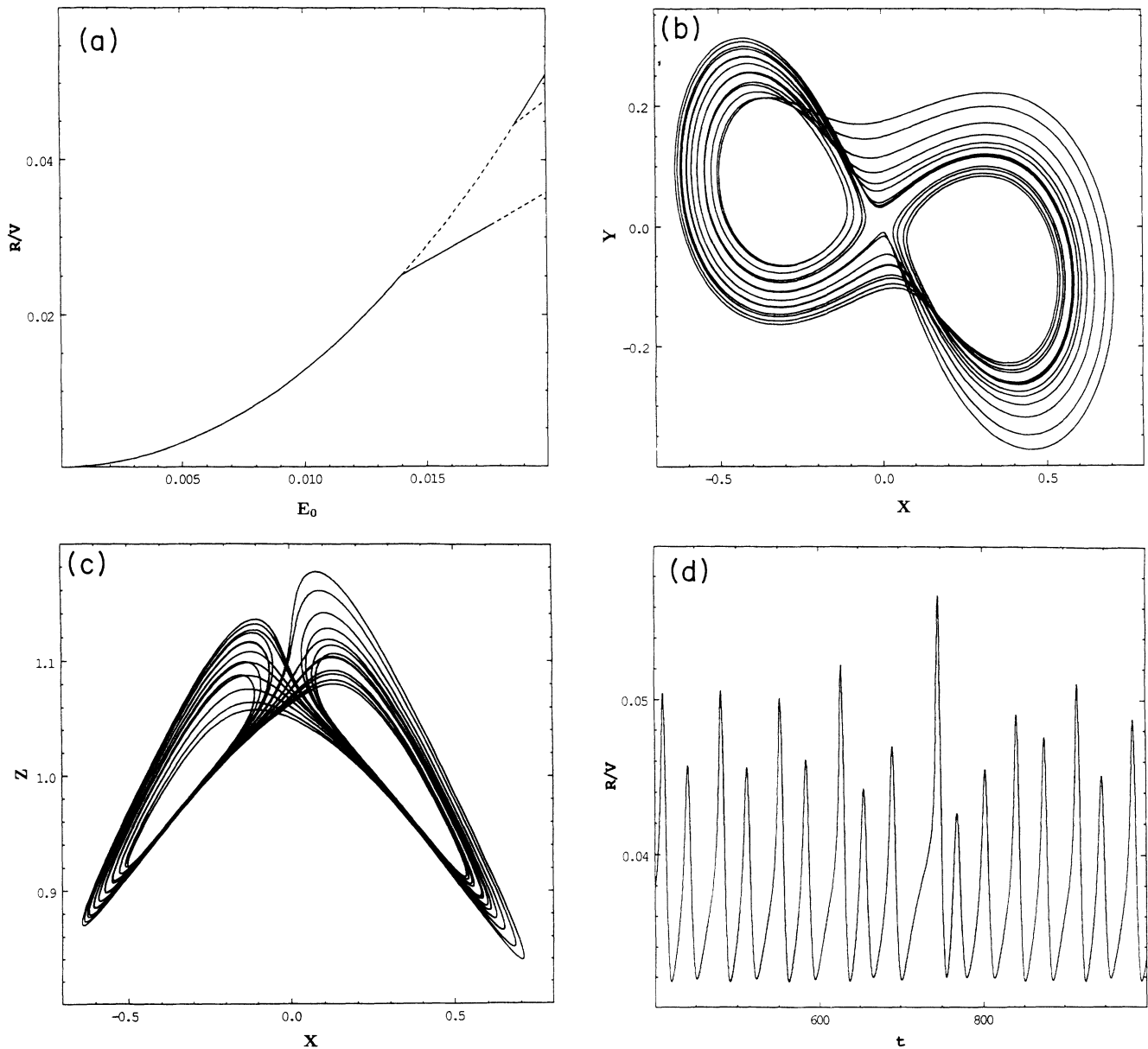


FIG. 2. (a) Dissipation rate vs electric-field curve as in Fig. 1(a), except that the mode selected is now *not* the first linearly unstable mode to appear as E_0 increases from zero. Notice the existence of a window, in which neither the axisymmetric nor helical fixed points are stable, just above $E_0 = 0.0175$. (b) X vs Y temporal behavior for $E_0 = 0.018$, for the situation shown in (a). (c) X vs Z behavior for the same situation as (a). (d) Dissipation vs time for the situation shown in (b) and (c).

(1)–(4) with any accuracy.

Figure 1(b) shows a typical relaxation (in the XY plane) to the helical fixed point for $E_0=0.11$, just above the appearance of the helical state. Figure 1(c) shows a similar relaxation in the XZ plane. Figure 1(d) is a computer-drawn surface $j_z=\text{const}=2.7$ for the associated helical state. The values of the quantities (indicated by the overbars) for the helical fixed point for $E_0=0.11$ are $\bar{X}=-0.11$, $\bar{Y}=-0.37$, $\bar{Z}=1.388$, $\bar{j}_0=2.5$, the dissipation per volume $R/V=\bar{j}_0 E_0=0.275 < E_0^2/\eta=0.303$.

While the behavior in Fig. 1 is typical of the behavior exhibited above the onset of linear instability, we may also obtain chaotic behavior by the following choice of parameters: $B_0=2.4$, $L_z=4\pi$, $a=\pi/2$, $\nu=\frac{1}{250}$, $\eta=7.8125 \times 10^{-3}$, $m=n=1$, $q=1$, and $\lambda a=4.522$. This set of mode numbers does *not* correspond to the first linearly unstable normal mode to appear for these parameters. Figure 2(a) is a dissipation versus E_0 curve similar to that shown in Fig. 1(a). However, notice that there is a “window” between approximately $E_0=0.0175$ and 0.0185 in which neither the axisymmetric state nor the helical state are stable. Figures 2(b) and 2(c) are XY and XZ plots indicating Lorenzian “strange attractor” behavior and no relaxation to any steady state. Figure 2(d) indicates the total dissipation versus time for this chaotic state. Interesting as it is, this behavior may perhaps be regarded as spurious, depending as it does on a physically unmotivated choice of the helical eigenmode for the Galerkin approximation.

IV. DISCUSSION

Our purposes here have included (i) setting out a computational scheme for future use in a many-mode numerical study of voltage-driven, dissipative MHD; and (ii) exploring the consequences of this scheme at the lowest nontrivial level of three-mode truncation. Of particular interest is the extent to which minimum-energy-dissipation rate principles^{6,7} may function as predictors of MHD states above thresholds for the onset of instability of the axisymmetric current profile.

The only numerical investigations reported here are the solutions of Eqs. (26)–(28) for the three-mode Galerkin approximation. The system bears a strong formal resemblance to the Lorenz equations and even becomes the Lorenz system for a particular choice of parameters. But its behavior is only chaotic if unphysical choices of modes are used in the truncation and/or if their limits as physically acceptable approximations to Eqs. (1)–(4) are exceeded. In physically motivated regimes, their behav-

ior is a relatively pedestrian relaxation to a steady state, either helical or axisymmetric. The helical states, having lower average total dissipation rate, are favored where the low-mode-number Galerkin approximation can be thought to be physical, in the region immediately above the axisymmetric stability boundary.

If, in fact, the solutions to Eqs. (26)–(28) do represent the physical behavior of the full set of Eqs. (1)–(4) better than they have a right to in the light of experience^{2,3} with the Bénard problem, we may ask why. We are uncertain as to the answer. For some problems we might summarize that there is perhaps some benefit to be obtained from using, as trial functions for the Galerkin approximation, true, physical, ordered eigenmodes from the associated continuum problem, rather than essentially arbitrarily chosen members of an orthonormal set not closely connected with the physics of the continuum problem. Few driven, dissipative physical problems of interest have the luxury of an explicitly calculable, analytically tractable set of eigenfunctions to describe the stability boundary, though as mentioned in the Introduction, the Lorenz problem is such a problem if free-slip (rather than no-slip) boundary conditions are assumed. In many cases, we simply do not know what would result if such a set of basis functions were used in a Galerkin approximation.

We should note that in the recent fluid turbulence work of Aubry *et al.*¹¹ and Sirovich,¹² for example, low-mode-number Galerkin approximations based upon the first few *statistically-arrived-at* eigenfunctions have met with some success in describing boundary layer measurements and turbulent computations of Ginzburg-Landau equation behavior. If the threshold behavior of our MHD system turns out to involve, as we believe it may, only a few Chandrasekhar-Kendall eigenmodes, presumably this would be reflected in the outcome of a similar systematic emergence of them from a Karhunen-Loeve procedure. Such possibilities await the results of a many-mode computation, which we are now pursuing. We should also note precursors of this present work in Maschke and Saramito,¹³ and in a Strauss approximation computation of Dahlburg *et al.*¹⁴ without, however, the present emphasis on the use of exact eigenfunctions as a Galerkin trial basis.

ACKNOWLEDGMENTS

This work was supported at Dartmouth College under U.S. Dept. of Energy Grant Nos. DE-FG02-85ER-53298 and DE-FG02-85ER-53194, and NASA Grant No. NAG-W-710.

¹E. Lorenz, *J. Atmos. Sci.* **20**, 130 (1963).

²J. H. Curry, *Commun. Math. Phys.* **60**, 193 (1978).

³J. H. Curry, J. R. Herring, J. Longcaric, and S. A. Orszag, *J. Fluid Mech.* **147**, 1 (1984).

⁴C. Canuto, M. Y. Hussaini, A. Quarteroni, and T. A. Zang, *Spectral Methods in Fluid Dynamics* (Springer-Verlag, New

York, 1987), Chap. 1.

⁵J. P. Dahlburg, D. Montgomery, G. D. Doolen, and L. Turner, *Phys. Rev. Lett.* **57**, 428 (1986); *J. Plasma Phys.* **37**, 299 (1987); **40**, 39 (1988).

⁶D. Montgomery and L. Phillips, *Phys. Rev. A* **38**, 2953 (1988).

⁷D. Montgomery, L. Phillips, and M. L. Theobald, *Phys. Rev.*

- A **40**, 1515 (1989).
- ⁸D. Montgomery, in *Trends in Theoretical Physics*, edited by P. J. Ellis and Y. C. Tang (Addison-Wesley, New York, 1990); Vol. I, pp. 239–262.
- ⁹X. Shan, H. Chen, and D. Montgomery, in *Proceedings of the Topical Conference on Research Trends in Nonlinear and Relativistic Effects in Plasmas, La Jolla, 1990*, edited by V. Stefan (AIP, New York, in press).
- ¹⁰S. Chandrasekhar and P. C. Kendall, *Astrophys. J.* **126**, 457 (1957); R. G. Storer, *Plasma Phys.* **25**, 1279 (1983).
- ¹¹N. Aubry, P. Holmes, J. L. Lumley, and E. Stone, *J. Fluid Mech.* **192**, 115 (1988).
- ¹²L. Sirovich, *Physica D* **37**, 126 (1988).
- ¹³E. K. Maschke and B. Saramito, *Phys. Scr.* **T2/2**, 410 (1982).
- ¹⁴J. P. Dahlburg, D. Montgomery, G. D. Doolen, and W. H. Matthaeus, *J. Plasma Phys.* **35**, 1 (1986).